Journal of Achievements in Materials and Manufacturing Engineering
VOLUME 29
ISSUE 1
July
2008

Microstructure, properties and hot deformability of the new maraging steels

S.J. Pawlak*, W. Zalecki
Institute for Ferrous Metallurgy, ul. K. Miarki 12-14, 44-100 Gliwice, Poland
* Corresponding author: E-mail address: spawlak@imz.pl

Received 09.04.2008; published in revised form 01.07.2008

Materials

ABSTRACT

Purpose: The effects of relevant metallurgical factors on the structure, fracture mode and properties of the high cobalt and cobalt free maraging steel has been studied. The aim was to better understand structure-property relations and enhance mechanical properties of the steels. To provide data needed for production and manufacturing technology, the high temperature deformability using physical simulation method was used.
Design/methodology/approach: To study structure-property relation, broad range of the experimental techniques was used: quantitative metallography, X-ray diffraction phase analysis, transmission electron microscopy and SEM fractography. The flow properties in the range of hot working processes were determined by physical simulation approach, using Gleeble 3800 system.
Findings: The cobalt-free maraging steel proved to be a valuable structural steel. At much higher fracture toughness it had only about 100 MPa lower yield stress, compared to that of high cobalt steel. Fracture surface morphologies were highly dependent on the steel grade and type of the mechanical test. The hot stress-strain characteristics were established for cobalt free maraging steel and compared to that of a stainless steel.
Research limitations/implications: To fully evaluate potential field of applications, deeper comparative studies of the high cobalt and cobalt-free maraging steels are needed, particularly fracture modes and service properties of some parts.
Practical implications: Very high mechanical properties and fracture toughness values obtained for the steels studied, make them suitable for advanced structural applications. The studies on the hot deformation behaviour of the steels are of practical value for the hot working process development.
Originality/value: Detailed evaluation of the metallurgical purity, microstructure and fracture modes, allowed for better understanding of the microstructure-property relationships in selected high strength steels. The results obtained are of practical value for the development, production and manufacture of the high strength maraging steels with improved properties.
Keywords: Metallic alloys; Maraging steels; Mechanical properties; Hot deformability; Microstructure

1. Introduction

In the development of the structural materials for the advanced applications, as in the aircraft industry, there is a constant strive to increase both strength and toughness. The best known ultrahigh strength steel grades (UHSS) - those with yield stress > 1400 MPa - are the quenched and tempered medium carbon low alloy Cr-Ni-Mo steels, having total alloy content limited to few percent. The other steels in the UHSS category, are the high nickel maraging steels, with the standard 18Ni-9Co-5Mo-Ti grade, often designated as MS250 [1-3]. High toughness and many technological advantages over the medium carbon low alloy steels, assured spreading of that steel, despite high price of the alloying elements. The salient step in the maraging steel development was introduction of the high cobalt AM100 (0.23C-11.5Ni-13.4Co-1.5Mo) grade. In the aged condition this steel has the yield strength well over 1700 MPa, at very high toughness [4-

6]. But this steel is very difficult to deform at room temperature, even in the annealed condition or after softening, what make it inconvenient in manufacture.

The recent trend in many industries, is to develop leaner and eco-friendly technology [7, 8]. For the steel development it means leaner compositions and fewer steps in manufacture. There seems to be a place for structural steel with better deformability, high toughness, admittedly somewhat lesser strength than 1700 MPa, but leaner composition. The cobalt free maraging steel of the 19Ni-4Mo-1Ti type is considered here as a promising composition.

Maraging steels - as all UHSS steels - are highly sensitive to nonmetallic inclusions, which are stress raisers and promote nucleation of voids and microcracks. In effect ductility and fracture toughness of the steel is reduced. To minimize the content of nonmetallic inclusions, the UHSS steels are typically melted under vacuum. In the UHSS steel production and manufacture a considerable degree of control is needed over many metallurgical factors, such as chemical composition, cleanliness, deformability, microstructure and heat treatment [9-18].

It is a common attitude in a new material investigation to look for a model describing its behaviour under high temperature deformation [19-22]. Thus the present study has both practical and research aspects. To find relations between metallurgical factors and fracture behaviour, the metallographic and fractographic analysis has been made for the case of cobalt free and high cobalt maraging steel.

The hot deformability was analysed as a next step of technology development, useful both for production and as an aid in manufacture. By physical simulation of the hot work processing, the flow curves (true stress vs. true strain curves) are determined. This data may then be applied to modelling and/or optimization of the hot working operations.

2. Material and methodology

2.1. Material

Most of the experiments were made with the 25-kg laboratory vacuum melted 19Ni-4Mo-1Ti and 0.23C-11.5Ni-13.4Co-1.5Mo maraging steels. The specimens for the mechanical and microstructural testing were prepared from forged 32 mm in dia. bars. Fracture toughness tests were conducted using fatigue precracked rectangular bars loaded in tension (a quasi-static test). At the tests, the plane-strain conditions were always preserved.

2.2. Methodology

Determination of the flow curves was carried out using Gleeble 3800 simulator. All tests (Axisymmetric Uniaxial Compression Testing) were performed according to DSI Inc. application notes [23,24], NPL instruction [25] and so far gained own experiences [26]. All specimens of diameter ϕ 10×12mm, were heated up to soaking temperature of 1100°C, at rate of 3°C/s. Soaking time was 60s. Afterwards specimens were cooled to deformation temperature at 10°C/s. Soaking time before deformation was 10s.

Strain and stress were automatically calculated according to following equations:

$$\varepsilon = \ln\left(\frac{h}{h_o}\right) \tag{1}$$

$$\sigma = \frac{4F}{\pi d^2} \tag{2}$$

where: h is final and h_o initial height of the specimen, d is current diameter of the specimen calculated from constant volume rule, F is force measured during test.

Lower limit of deformation temperature range was determined performing dylatometry measurements, using DIL805A/D dilatometer.

Tests were carried out according to following conditions:

- deformation temperatures: 1100°C, 950°C, and 800°C,
- strain rates: $0.1s^{-1}$; $1.0s^{-1}$, and $10s^{-1}$.

All specimens were compressed up to (constant) strain of -1.0. Afterwards they were cooled down to room temperature in compressed air. Deformation was done using ISO-T tungsten carbide anvils. Nickel based grease and graphite foil were used for lubrication.

For preprocessing and final correction of flow curves „Opty_axi" program was used. „Opty_axi" is FEM based software, specially designed for Gleeble recorded data analysis, it uses inverse analysis [26-29] for identification of rheological parameters [30]. The preprocessing comprised data file cutting (unnecessary data are removed) and data filtering. The other feature of the programme is possibility to determine the process activation energy ***Q*** and strain rate sensitivity index ***m***. After preprocessing data files were used to calculate corrected stress-strain curves to eliminate the non-uniform distribution of strain and strain rate caused by friction phenomena and non-uniform temperature field.

3. Results and discussion

3.1. Microstructure and properties

To efficiently measure geometric parameters of very small inclusions in very pure steels, a special method has been developed, using digital quantitative image analyzer [31].

Table 1.
Geometrical parameters of the inclusions in the Co-free ϕ32 mm laboratory forging (inclusion content - 0.086% vol.)

Parameter	Mean µm	Std. dev. µm	Min. µm	Max. µm
Equivalent dia.	1.05	0.53	0.46	3.75
Length	1.54	1.08	0.52	9.37
Thickness	0.60	0.28	0.21	1.86
Aspect ratio	2.72	2.09	1.06	20.33

Table 2.
Geometrical parameters of the inclusions in the high cobalt ϕ32 mm laboratory forging (inclusion content - 0.022% vol.)

Parameter	Mean µm	Std. dev. µm	Min. µm	Max. µm
Equivalent dia.	0.84	0.41	0.27	3.02
Length	1.05	0.72	0.41	8.47
Thickness	0.54	0.25	0.14	1.70
Aspect ratio	1.96	0.70	1.05	10.02

Mean volume fractions of inclusions the Co-free and the high cobalt heats were 0.086% and 0.022%, respectively. The common geometrical parameters of the inclusions in the forged steels are shown in Table 1 and 2. Analogous measurements were also made for two foreign industrial melts of the aircraft quality [32], which showed that the purity (0.056 vol. % on average), was comparable to that of the laboratory melts (avg. 0.054 vol. %).

a)

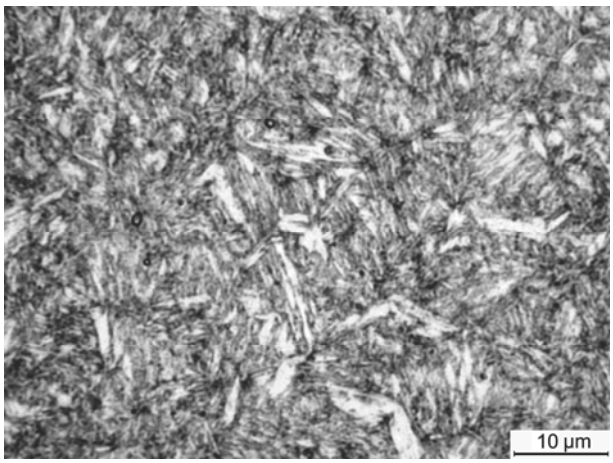

b)

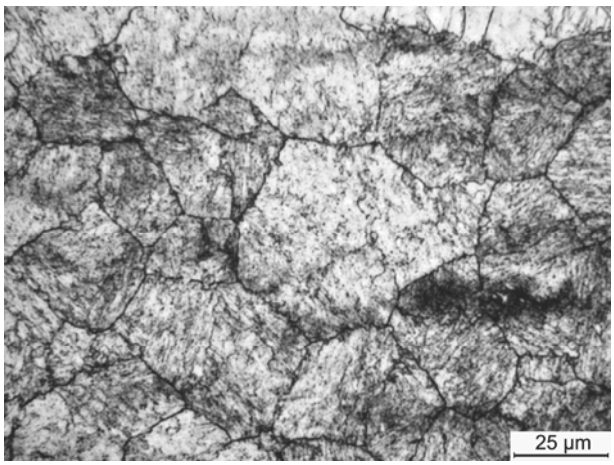

Fig. 1. Micrographs of the aged high cobalt (a) and the Co-free steel (b)

Light microscopy after full heat treatment, Fig.1, shows lath martensite microstructure in both steels. The low cobalt steel had much higher grain size than high cobalt steel. The transmission electron micrograph (TEM), Fig. 2a, shows the lath substructure of martensite with high dislocation density in the unaged high cobalt steel. Study of the aged steels at high magnifications, Fig. 2b, revealed very small precipitates, but electron diffraction attempts to identify their crystal structure were unsuccessful. Other attempt to identify the particles present in the steel after full heat treatment, was the X-ray diffraction of the chemically extracted residues. On the diffraction pattern of the high cobalt steel the reflections from hexagonal Mo_2C carbides were observed and also from MoC (also hexagonal). In the case of Co-free steel the basic constituent of the residues was the Fe_2Mo intermetallic phase, the NiTi, Ni_3Ti, and TiC were also identified.

The mechanical properties of the steels after full heat treatment are presented in Table 3.

a)

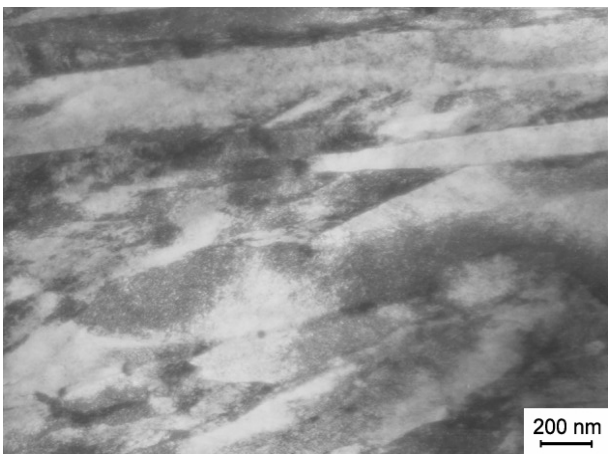

b)

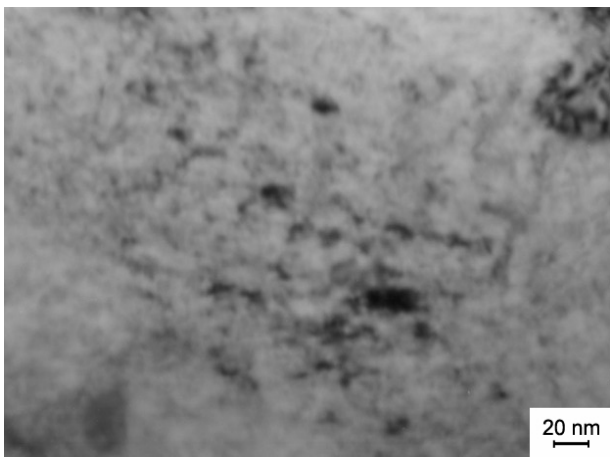

Fig. 2. TEM micrograph of the aged high cobalt steel showing lath martensite (a) and precipitates in martensitic matrix (b)

Table 3.
Mechanical properties and toughness of the aged steels

Steel	YS MPa	UTS MPa	R.A. %	Charpy J	K_{1c} MPa·m$^{1/2}$
High cobalt	1716	1912	53	39	70.1 ±5.5
Co-free	1624	1705	48	15	82.3 ±1.6

The heat treatment of the Co-free steel involved annealing and ageing. In the case of high cobalt steel, the refrigeration treatment at -78°C for about 2.5 hrs was applied after annealing, because the retain austenite was occasionally observed. Both steels were aged at 480°C for 3 hrs.

The cobalt-free maraging steel, has only about 100 MPa smaller yield strength, but much higher fracture toughness K_{1c} value than the high-Co steel. To compare the steels, taking into account both strengths and toughness, "the structural efficiency" parameter, defined as $(K_{1c}/YS)^2$ was used. The structural efficiency parameter, having a unit of mm, is directly proportional do the allowable crack size - what results from linear elastic fracture mechanics. In the Fig. 3, the black points with spread bars, are fracture toughness values, while square points with two characters inside, represent the "structural efficiency" parameters - values of which to be read on the right side of the figure. Based on this criterion, the Co-free steel seems to be better than the high cobalt grade, Fig. 3, but definite judgment could only be made, when crack detection and inspection system was considered.

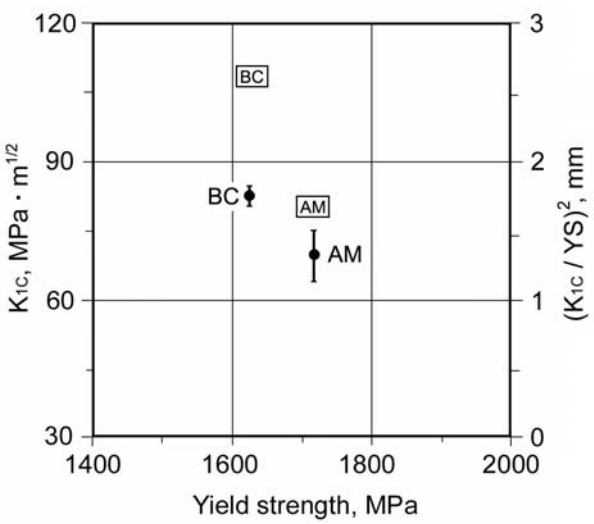

Fig. 3. Fracture toughness and the "structural efficiency" of the Co-free steel, BC, and the high cobalt steel, AM (square points with two characters inside refer to the right side axis - see text for explanation)

Fracture surface examination by scanning electron microscopy, made to explain differences in the mechanical and fracture properties of the steels, resulted in the following observations. In the tensile tested specimens, the fully ductile fractures with characteristic very deep voids were observed in both steels. In other tests of the aged steels (fully hardened condition) the fracture surfaces were very sensitive to the steel grade and the mechanical test, i.e. precracked quasi-static bending and impact bending (Charpy-V).

The fracture surfaces of the fracture toughness (K_{1c}) specimens of the high cobalt steel were flat, made of shallow ductile micro voids, Fig. 4a, and occasionally intercrystalline tears were seen. In case of the Co-free steel fracture surfaces were more complicated. Apart from ductile areas, large part of the surface was essentially intercrystalline, but with not clearly developed microsurfaces of the grain size facelets, Fig. 4b. These facelets were often connected by ductile transcrystalline shears.

a)

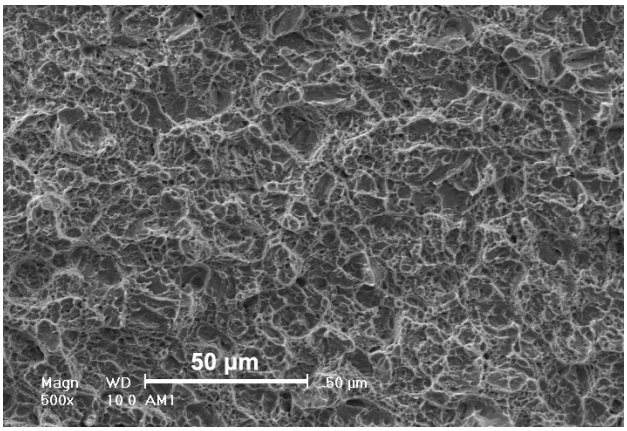

b)

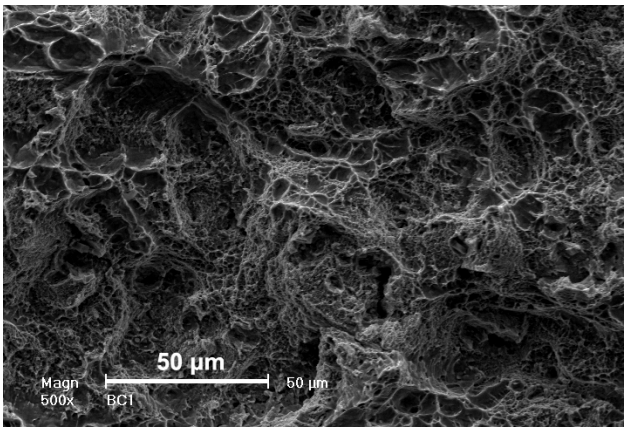

Fig. 4. SEM fractograph of the K_{1c} specimens of the high cobalt (a) and the Co-free steel (b)

The surfaces of K_{1c} tested specimens were so flat and uniform that profilometric measurements could be made using the Taylor-Hobson instrument. Roughness values, Ra, for the high cobalt and the Co-free steel, were 4.3 µm and 10.3 µm respectively. Much more rough and less uniform were surfaces in the Charpy-V impact tested specimens, because the intercrystalline fracture constituents were present in both steels, particularly in the cobalt-free steel. The work is in progress on the fracture mode implications for the service properties of the parts made of the steels studied.

3.2. Hot deformability

For different deformation temperatures and strain rates, the flow stress values during upsetting of cylindrical specimen was calculated using recorded force values. Figures 5, 6 and 7 show example flow curves for the cobalt-free (BC) steel, based on raw data. The stress-strain curves were drawn for different strain rates and separately for each deformation temperature. The flow curves for the ph13-8 stainless steel were similar, but maximum stress values were lower then for the cobalt-free steel. The curves shown in Figs. 5-7 indicate the drop in maximum flow stress values with increase of deformation temperature.

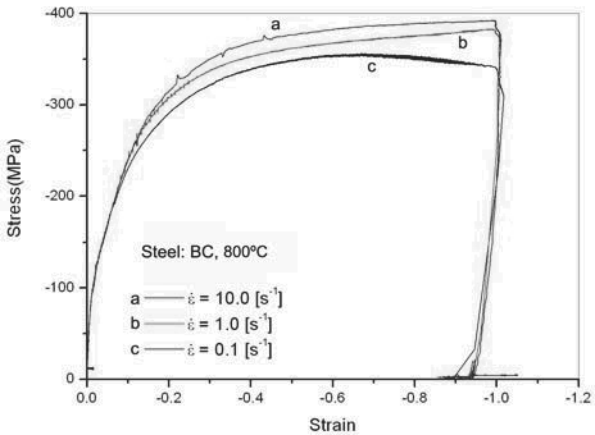

Fig. 5. Experimental true stress-true strain curve of the cobalt-free steel compressed at 800°C, and at different strain rates

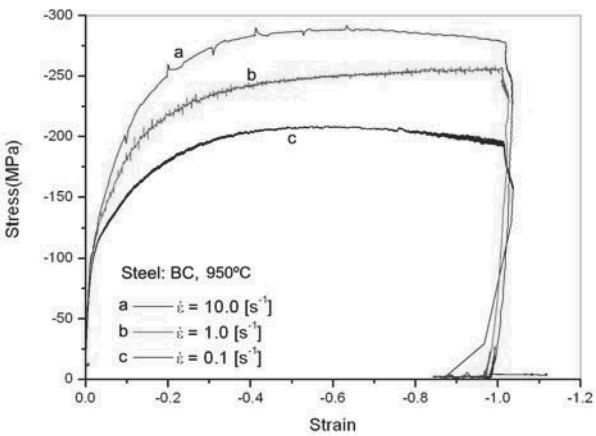

Fig. 6. Experimental true stress-true strain curve of the cobalt-free steel compressed at 950°C, and at different strain rates

Raw data seems to indicate that susceptibility of the material to strain rate increases with temperature rise. For better understanding of the maraging steel behaviour during hot deformation, the raw data were corrected (preprocessing step) to eliminate the influence of temperature rise during deformation and non-uniform distribution of strain and strain rate. The determined activation energy ***Q*** and strain rate sensitivity index ***m*** values for the stainless steel and cobalt - free steels were ***Q***=33252 J/mol, ***m***=0.068, and ***Q***=34729 J/mol, ***m***=0.115, respectively.

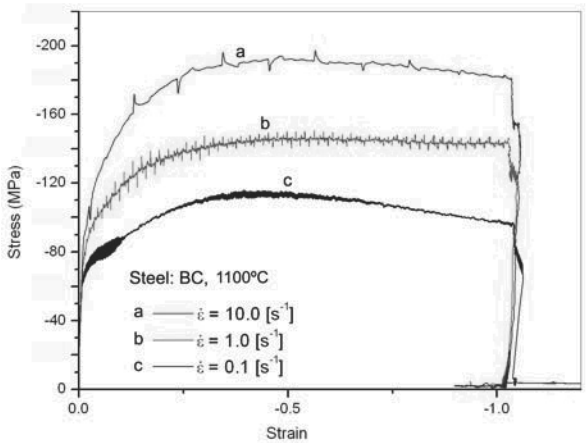

Fig. 7. Experimental true stress-true strain curve for of the cobalt-free steel compressed at 1100°C, and at different strain rates

As it was stated earlier Opty_axi programme enables correction of flow curves to eliminate the non-uniform distribution of strain and strain rate caused by friction phenomena and non-uniform temperature field.

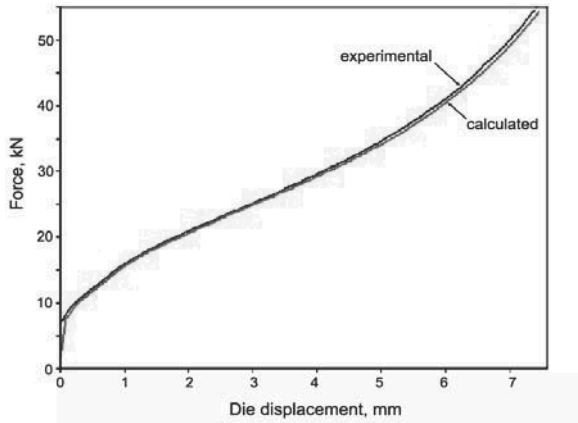

Fig. 8. Force vs. displacement of the cobalt-free steel compressed at temperature of 950°C, and at strain rate of 1.0 s^{-1}

An example of comparison of measured and calculated force after correction is shown in Fig. 8. In all cases, for both steels studied here, the fitting results were very good. The stress-strain curves experimentally gained (square points) and after correction (circle points), for the cobalt-free steel are shown in Fig. 9-12.

The analysis of hot processing results demonstrated that the cobalt-free maraging steel have similar hot characteristics as the ph13-8 stainless steel, but has maximum stress level roughly 50 MPa higher, for each strain rate and temperature studied. Both steels were highly susceptible to deformation temperature (e.g. Fig. 9 and 11) and strain rate (e.g. Fig. 11 and 12). Within the range of temperatures studied, the effect of strain rate on the maximum stresses measured at strain rates of 0.1 and 10 s-1, was such that the differences in the maximum stresses were roughly constant (at 100 MPa).

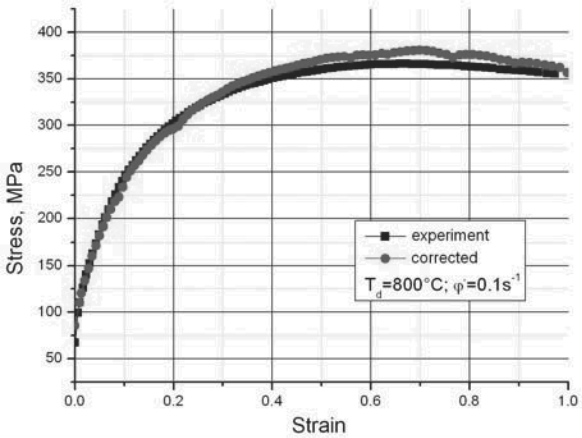

Fig. 9. Stress-strain curves of the cobalt-free steel compressed at temperature of 800°C, and at strain rate of 0.1 s^{-1}

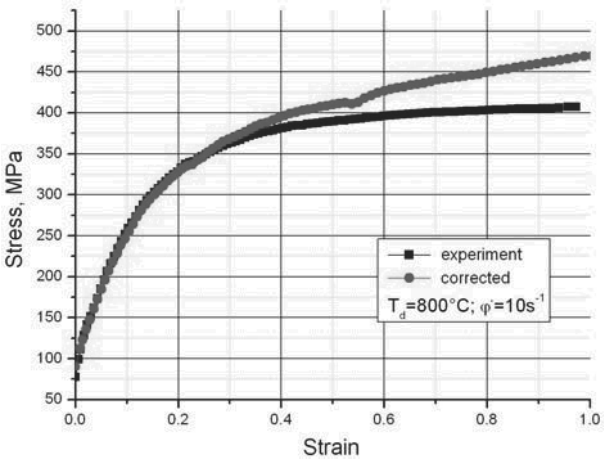

Fig. 10. Stress-strain curves of the cobalt-free steel compressed at temperature of 800°C, and at strain rate of 10 s^{-1}

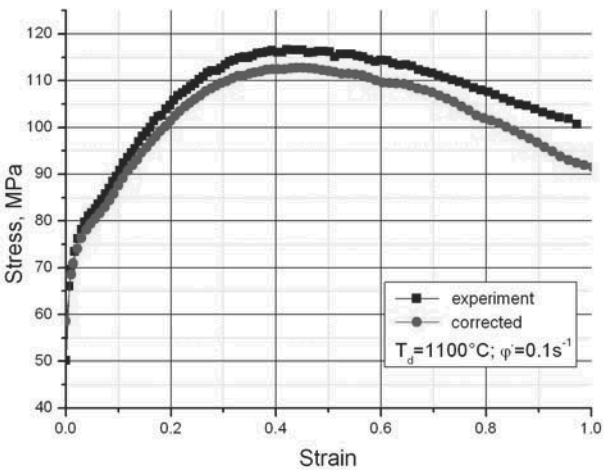

Fig. 11. Stress-strain curves of the cobalt-free steel compressed at temperature of 1100°C, and at strain rate of 0.1 s^{-1}

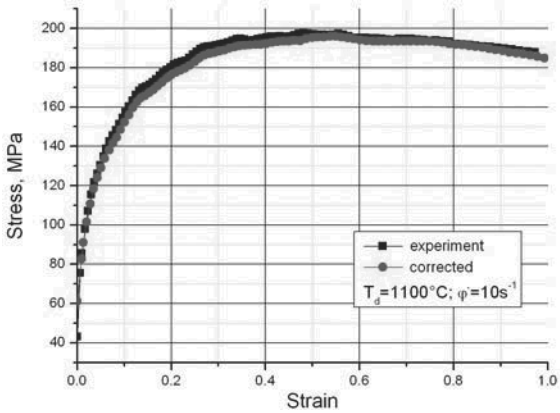

Fig. 12. Stress-strain curves of the cobalt-free steel compressed at temperature of 1100°C, and at strain rate of 10 s^{-1}

For numerical modelling of hot work processing of the steels, the development of the constitutive model is necessary. Microstructure changes in specimens subjected to deformation at 800°C and 1100°C were shown in Fig. 13. The observations of microstructure confirm flow curves analysis results. The grains in the specimen deformed at 800°C showed pancake form, Fig. 13a, whereas after deformation at 1100°C at strain rate 10s^{-1} the structure is partly recrystallized, Fig. 13b.

a)

b)

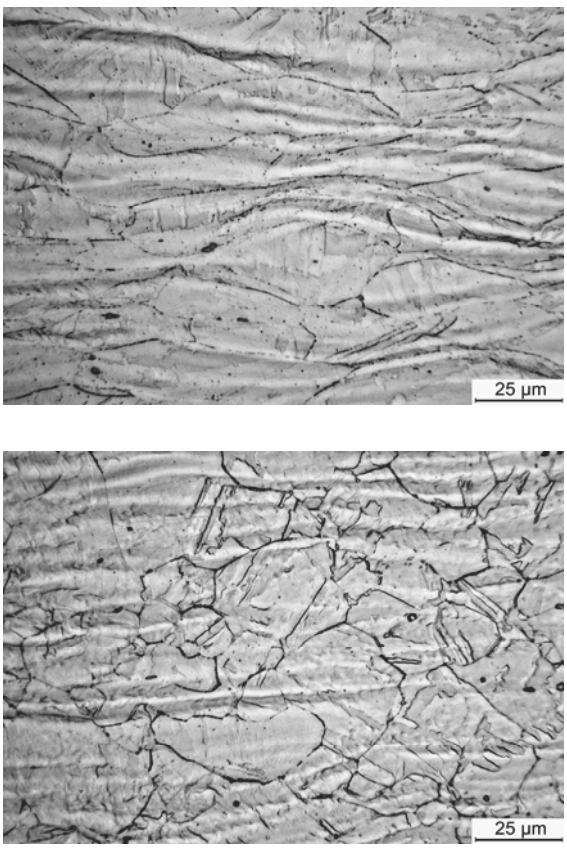

Fig. 13. Microstructure of the cobalt-free steel after hot deformation; a) at temperature of 800°C, and strain rate of 0.1s^{-1}, b) at temperature of 1100°C, and strain rate of 10s^{-1})

4. Conclusions

The laboratory vacuum melted maraging steels, cobalt-free 19Ni-4Mo-1Ti and high cobalt 0.23C-11Ni-13Co-1.5Mo grades have been studied. Due to retained austenite observed in the high cobalt steel, after annealing the refrigeration heat treatment was applied to this steel. Both steels were aged at 480 °C. After full heat treatment both steels showed very high yield stress and plain strain fracture toughness of over 1600 MPa and 70 MPa·m$^{1/2}$, respectively. Very high mechanical properties combined with other technological merits makes the steels studied suitable for advanced structural applications. When both steels are compared on the bases of "the structural efficiency" - a factor combining both yield stress and K_{1c} values - the cobalt-free maraging steel seems to be better. Non-metallic inclusions content in the Co-free maraging steel was much higher than in high cobalt steel. On average, the cleanliness of the laboratory vacuum melted steels was comparable to that of the foreign industrial steels of the aircraft quality.

The SEM fracture surface morphologies of the aged tensile tested specimens were fully ductile. In other tests, i.e. Charpy-V and plain stress fracture toughness, the fracture surfaces were highly dependent on the steel grade and type of the mechanical test. In the high cobalt steel the fractures were generally more ductile and more flat than in the cobalt-free steel. Deeper study in the fracture mode characteristics is needed to better understand differences in fracture phenomena of the steels studied.

The physical simulation of the hot processing demonstrated high susceptibility to deformation temperature (800 to 1000°C) and strain rate (0.1 to 10 s^{-1}). The cobalt-free maraging steel have similar hot characteristics as the stainless steel (ph13-8 grade), but has maximum stress roughly 50 MPa higher, for each strain rate and temperature studied. Within the range of temperatures studied, the effect of strain rate on the maximum stresses measured at strain rates of 0.1 and 10 s^{-1}, was such that the differences in the maximum stresses were roughly constant (at 100 MPa).

Acknowledgements

This work was supported by the Polish Ministry of Science and Higher Education, grant No. R07 034 02.

References

[1] Standard SAE AMS 6514 C, 1992, "Steel maraging, bars, forging, tubing and rings 18.5 Ni - 9.0 Co - 0.65 Ti - 0.10 Al Consumable Electrode Vacuum Melted, Annealed".

[2] S.J. Pawlak, Correlation between ductility and the second phase particles parameters in vacuum melted maraging steels, Proceedings of the International Symposium on Metallography, Strbske Pleso, Slovakia 3 (1986) 26-30.

[3] Z. Kędzierski, A. Zielińska-Lipiec, Charpy toughness anisotropy of maraging steels, Hutnik 54/ 6 (1987) 182-186 (in Polish).

[4] H. Everson, Advanced engineering steels for aerospace, Materials World, 1994, 461-462.

[5] W.M. Garrison Jr., M.A. Rhoads, An evaluation of an ultra-high strength steel strengthened by alloy carbide and intermetallic precipitates, Transactions of the Indian Institute of Metals 49/3 (1996) 151-162.

[6] Th.J. McCaffrey, Combined strength and toughness characterize new aircraft alloy, Advanced Materials and Processes 142/3 (1992) 47-50.

[7] S.J. Pawlak, Microstructure and properties of vacuum melted high cobalt and cobalt-free maraging steels, Journal of Achievements in Materials and Manufacturing Engineering 27/1 (2008) 31-34.

[8] M. Ahmed, I. Salam, F.H. Hasmii, A.Q. Khan, Influence of banded structure on the mechanical properties of a high-strength maraging steels, Journal of Materials Engineering and Performance 6/2 (1997) 165-171.

[9] A.A. Ezow, Fracture types in structural steels, Metal Science and Heat Treatment 4 (2004) 34 (in Russian).

[10] N.G. Orekhov, E.B. Chabina, I.P. Zhegina, L.N. Belyakov, The destructive mechanisms in high-strength steels under the effect of impurities, Metal Science and Heat Treatment 37/1 (1995) 10-15 (in Russian).

[11] Y. Katz, N. Tymiak, W.W. Gerberich, Local approach contributions into the global view of the mechanical crack-tip environment formulation, Journal of Achievements in Materials and Manufacturing Engineering 24/1 (2007) 162-165.

[12] L.A. Dobrzański, Metal Engineering Materials, WNT, Warsaw, 2004 (in Polish).

[13] J. Trzaska, L.A. Dobrzański, A. Jagiełło, Computer programme for prediction steel parameters after heat treatment, Journal of Achievements in Materials and Manufacturing Engineering 24/ 2 (2007) 171-174.

[14] P. Bała, J. Pacyna, J. Krawczyk, The kinetics of phase transformations during tempering of Cr-Mo-V medium carbon steel, Journal of Achievements in Materials and Manufacturing Engineering 20 (2007) 79-82.

[15] S.J. Pawlak, Austenite stability in the high strength metastable stainless steels, Journal of Achievements in Materials and Manufacturing Engineering 22/2 (2007) 91-94.

[16] M. Hetmańczyk, L. Swadźba, B. Mendala, Advanced materials and protective coatings in aero-engines applications, Journal of Achievements in Materials and Manufacturing Engineering 24/1 (2007) 372-381.

[17] L.A. Dobrzański, Engineering materials and material design, Principles of materials science and physical metallurgy, WNT, Warsaw, 2006 (in Polish).

[18] Technological Cooperation Forum - Pratt and Whitney Canada, Warsaw, 2006 (Warsaw Technical University).

[19] N. Wolańska, A.K. Lis, J. Lis, Investigation of C-Mn-B steel after hot deformation, Archives of Materials Science and Engineering 28/2 (2007) 119-125.

[20] K. Ducki, Structure and precipitation strengthening in a high temperature Fe-Ni alloy, Archives of Materials Science and Engineering 28/4 (2007) 203-210.

[21] M. Opiela, Thermo-mechanical treatment of the C-Mn steel with Nb, Ti, V and B microadditions, Archives of Materials Science and Engineering 28/6 (2007) 377-380.

[22] B. Koczurkiewicz, The model of prediction of micro-structure austenite C-Mn steel, Archives of Materials Science and Engineering 28/7 (2007) 421-424.

[23] Application Note: Axisymmetric Uniaxial Compression Testing Using ISO-T Anvils on Gleeble Systems.
[24] GLEEBLE® 3500/3800 Options Reference Manual 2/98 N320, Chapter: Hot Deformation Options, Dynamic Systems Inc., 1996-1998.
[25] Measuring Flow Stress in Hot Axisymmetric Compression Tests, Revised Report National Physical Labolatory,– Summer 2002.
[26] R. Kuziak, W. Zalecki, Z. Lapczynski, Physical simulation of metallurgical processes using Gleeble system, Institute for Ferrous Metallurgy, Report No S-00312/1/BM 2000 (in Polish).
[27] D. Szyndler, Inverse problem in the process parameters identification of metal plastic deformation, Ph.D. dissertation, AGH, Kraków, 2001(in Polish).
[28] A. Gavrus, E. Massoni, J.L. Chenot, An Inverse Analysis Using a Finite Element Model for Identification of Rheological Parameters, Journal of Materials Processing Technology 60 (1996) 447-454.
[29] J.G. Lenard, M. Pietrzyk, L. Cser, Mathematical and Physical Simulation of the Properties of Hot Rolled Product, Elsevier, Amsterdam, 1999.
[30] T. Kondek, D. Szeliga, M. Pietrzyk, Computer software for the identification of reological parameters based on axisymmetric compression test, Proceedings of the 10th Conference "Informatics in Metals Technology" KomPlasTech'2003, Wisła–Jawornik, 2003, 207-214.
[31] S.J. Pawlak, A. Maciosowski, J. Janiczek, J. Wiedermann, Development and implementation of quantitative metallographic testing methodology using digital image analyzer, IMZ Reports 1 (2006) 54-56 (in Polish) .
[32] S.J. Pawlak, A. Maciosowski, J. Gazdowicz, Development of quantitative methods of the inclusion analysis with application to high purity high alloy steels, IMZ Reports, 2008 (in print).